Available online at www.sciencedirect.com
ScienceDirect
Polymer 47 (2006) 7361–7367
polymer
www.elsevier.com/locate/polymer

Hybrid composites of conductive polyaniline and nanocrystalline titanium oxide prepared via self-assembling and graft polymerization

Jing Li [a], Lihua Zhu [a,*], Yinghui Wu [a], Yutaka Harima [b], Aiqing Zhang [c], Heqing Tang [a,*]

[a] *Department of Chemistry, Huazhong University of Science and Technology, 1037 Luo-Yu Road, Hong-Shan Qu, Wuhan, Hubei 430074, People's Republic of China*
[b] *Department of Applied Chemistry, Graduate School of Engineering, Hiroshima University, 1-4-1 Kagamiyama, Higashi-Hiroshima 739-8527, Japan*
[c] *Hubei Key Laboratory for Catalysis and Material Science, College of Chemistry and Material Science, South-Central University for Nationalities, Wuhan 430074, People's Republic of China*

Received 14 February 2006; received in revised form 19 August 2006; accepted 23 August 2006
Available online 8 September 2006

Abstract

After TiO_2 nanoparticles were surface modified, conductive polyaniline (PANI) layer was chemically grafted on the surface of the self-assembled monolayer (SAM) coated TiO_2 nanoparticles, resulting in PANI/SAM-TiO_2 composites. In the preparation process of the hybrid composites, γ-aminopropyltriethoxysilane was used as a coupling agent to form a dense aminopropylsilane monolayer with active sites for the graft polymerization of aniline. The resulted composite nanoparticles were characterized by using TEM, FTIR, TGA, and UV–vis-diffuse reflectance spectroscopy. The thermogravimetric analysis confirmed that the inserted SAM layer improved the thermal stability of the PANI–TiO_2 nanocomposites. Compared with neat-TiO_2 nanoparticles without any surface modification, moreover, the PANI/SAM-TiO_2 nanocomposites showed better photocatalytic activity in photodegradation of methyl orange under sunlight, which was partly attributed to the sensitizing effect of PANI.

Keywords: Self-assembled monolayer; Graft polymerization; Polyaniline–titania hybrid

1. Introduction

In recent years, nanocomposites of conductive polymers and inorganic particles have attracted more and more attention, since they have interesting physical properties and many potential applications [1–4]. However, conducting polymers are not molten in nature and generally insoluble in common solvents, thus it is difficult to prepare conducting polymer/inorganic nanoparticle composites by conventional blending or mixing in solution or melt form. Encapsulation of inorganic nanoparticles inside the shell of conducting polymers is a feasible way of preparing conductive polymer/inorganic particle nanocomposites. Several metals and metal oxides in particles have so far been encapsulated into the shell of conducting polymers giving rise to a host of nanocomposites [5–10]. The physical and chemical properties of composites may be tuned by selecting the types of the polymers and the inorganic nanoparticles. For example, composites of conductive polyaniline (PANI) and nanocrystalline TiO_2 combine the merits of both PANI and TiO_2 particles, having potential applications in conductive coating, charge storage, electrocatalysis, electrochromic devices and photovoltaic cells.

At the present time, several approaches of preparing PANI/TiO_2 nanocomposite have been reported. Yoneyama got a nanocomposite film by electrochemical deposition of TiO_2 particles (~22 nm) into PANI film, and succeeded in writing with UV light on PANI film [11]. Somani and coworkers prepared highly piezoresistive PANI/TiO_2 composites by in situ polymerization of aniline in the presence of fine-grade

* Corresponding authors. Tel.: +86 27 87543432; fax: +86 27 87543632.
E-mail addresses: lhzhu63@yahoo.com.cn (L. Zhu), hqtang62@yahoo.com.cn (H. Tang).

0032-3861/$ - see front matter © 2006 Elsevier Ltd. All rights reserved.
doi:10.1016/j.polymer.2006.08.059

powders of anatase TiO_2 (~100 nm) [12]. Xia and Wang obtained core-shell-structured PANI/TiO_2 composites through chemical polymerization of aniline in the presence of TiO_2 particles under ultrasonic irradiation [8]. Zhang and Wan synthesized PANI/TiO_2 composite nanotubes by in situ polymerization in the presence of TiO_2 nanoparticles and β-naphthalenesulfonic acid as both the dopant and the template [13]. Xiong et al. obtained PANI/TiO_2 bilayer microtubes by using anodic aluminum oxide membrane with ordered pore structure as template [14]. In all these cases, however, PANI adheres to TiO_2 particles via physical adsorption, being unfavorable to the stability of the composites.

It is expected that a direct chemical bonding of PANI chains onto TiO_2 surface will improve the chemical stability of PANI/TiO_2 composites. The surface-initiated graft polymerization in conjunction with a self-assembling technique is a useful synthetic route to precisely design and functionalize the surfaces of various solid materials by well-defined polymers and copolymers [15–20]. Its key advantage is that the surface of the materials can be modified or tailored to acquire very distinctive properties through the choice of different grafting monomers, while maintaining the substrate properties. It also ensures an easy and controllable introduction of graft chains with a high density and exact localization onto the surface. Compared with the physically coated polymer chains, the covalent attachment of the grafted chains onto a material surface avoids the desorption of the chains and maintains a long-term chemical stability of the introduced chains [21]. Li and Ruckenstein used the surface graft polymerization of aniline on photopatterned self-assembled phenylsilane monolayers to generate well-defined patterns of PANI on a planar Si (100) surface [22]. In the present work, we use γ-aminopropyltriethoxysilane to form a self-assembled monolayer (SAM) on the surface of TiO_2 nanoparticles, which allows a further surface oxidative graft polymerization to form a dense PANI layer. Along with being characterized, the thermochemical stability and the photocatalytic activity under sunlight of the obtained PANI/TiO_2 composites have also been evaluated.

2. Experimental section

2.1. Materials

Anatase TiO_2 nanoparticles with average particle size of 15 nm were obtained from Zhoushan Nano-materials Co., Ltd. γ-Aminopropyltriethoxysilane was obtained from Organosilicane Chemical Company of Wuhan University. The other chemicals were bought from Tianjin Chemical Reagent Co., Ltd., and were of analytical grade. All the chemicals were used as received, except for aniline, which was fractionally distilled under reduced pressure, and stored at low temperature prior to use.

2.2. Preparation of PANI/SAM-TiO_2 nanocomposites

A graft polymerization on a solid surface often requires a pre-immobilization of initiator and/or coupling agent, which is easily achieved by the self-assembled monolayer-deposition method [22,23]. Our approach to prepare PANI/SAM-TiO_2 nanocomposites consisted of two major steps. As shown in Fig. 1, the first step was to prepare SAM-coated TiO_2 nanoparticles (SAM-TiO_2), and the second step was grafting PANI onto the SAM-coated TiO_2 nanoparticles. In the first step, neat-TiO_2 nanoparticles were first exposed to water vapor (100 °C) for about 3 min to generate a particle surface with high coverage of Ti–OH groups, followed by a drying at 120 °C. After the water vapor treatment, the nanoparticles were dispersed into a solution of γ-aminopropyltriethoxysilane in ethanol (about 10 mmol L^{-1}) under a nitrogen

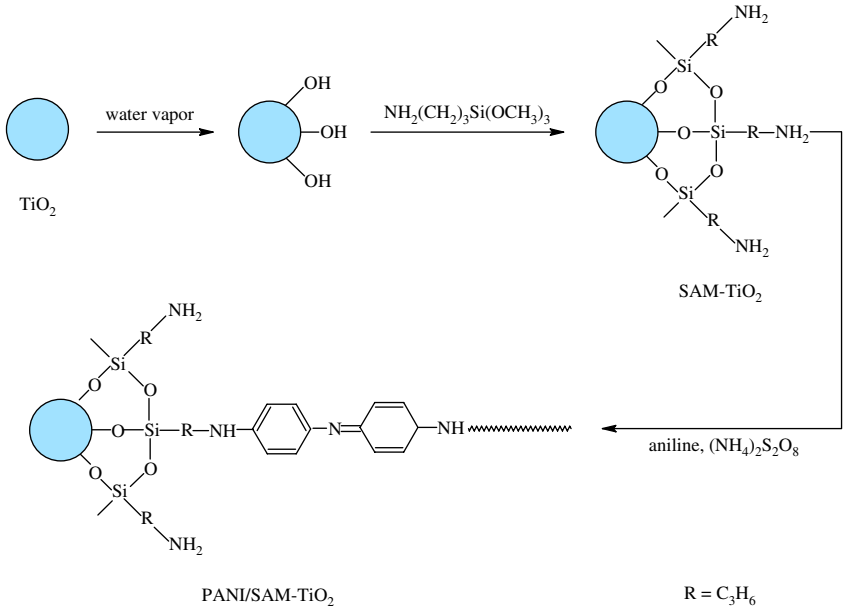

Fig. 1. Schematic on preparation routes of PANI/SAM-TiO_2 composites.

atmosphere, sonicated for 15 min, held at room temperature for 24 h, and then washed with ethanol in an ultrasonic bath to remove the unreacted γ-aminopropyltriethoxysilane. The SAM-coated TiO_2 nanoparticles were removed from the nitrogen atmosphere, collected by filtration, rinsed successively with ethanol, and finally dried.

In the second step, about 0.4 g SAM-coated TiO_2 nanoparticles were dispersed into 25 mL of 0.1 mol L^{-1} HCl aqueous solution of aniline with ultrasonic vibrations for 15 min. After that, 10 mL aqueous solution of ammonium peroxydisulfate (APS) was added dropwise within 15 min under stirring at room temperature, and the mixture was allowed to polymerize under stirring for another 4 h, resulting in PANI in its emeraldine (EM) salt state. The EM salt grafted nanoparticles were rinsed with distilled water, and were subsequently washed several times in *N*-methylpyrrolidinone (NMP) in order to remove any physically adsorbed EM base. Then, the solution was centrifuged and the PANI/SAM-TiO_2 nanoparticles were obtained by filtration. The nanoparticles were washed with alcohol, followed by washing with distilled water to remove any residual NMP and then by a drying under reduced pressure. In the experiment, the initial molar ratios of aniline to APS were kept at 1:1. Two initial concentrations of aniline (i.e., 2.5 and 10 mmol L^{-1}) were used to obtain TiO_2 nanoparticles capped with PANI layers of different thicknesses. In this way, two types of PANI/SAM-TiO_2 nanoparticles were prepared, being referred to as PANI-2.5/SAM-TiO_2 and PANI-10/SAM-TiO_2, respectively.

2.3. Preparation of PANI/neat-TiO_2 nanocomposites

As a control, PANI/neat-TiO_2 composite nanoparticles were also prepared by using chemical oxidative polymerization of aniline in the presence of as-received TiO_2 particles without the vapor pretreatment and SAM coating, the resultant composite nanoparticles were referred to as PANI-10/neat-TiO_2.

2.4. Characterizations

Morphology of all samples was observed on a Tecnai G2 20 TEM instrument (FEI). Fourier transform infrared (FTIR) spectra were obtained with a resolution of 4 cm^{-1} in the range 400–4000 cm^{-1} by using a VERTEX 70 spectrometer (Bruker). Measurements were performed in the transmission mode in spectroscopic grade KBr pellets for all the powders. Thermogravimetric analysis (TGA) was carried out on a TGS-2 instrument (Perkin–Elmer) at a heating rate of 20 °C min^{-1} in air. A UV-2550 scan UV–vis spectrophotometer (Shimadzu) equipped with a Labsphere diffuse reflectance accessory was used to obtain the reflectance spectra, using $BaSO_4$ as a reflectance reference.

2.5. Measurement of photocatalytic activities

Photocatalytic activities of the obtained nanocomposites and neat-TiO_2 nanoparticles were evaluated by monitoring photodegradation of methyl orange (MO) in aqueous solution containing. A 50 mg portion of nanoparticles was dispersed into 250 mL of the aqueous MO solution (10 mg L^{-1}) in optically matched Pyrex vessel. Under stirring, the mixed solution was irradiated under sunlight. After a certain period of irradiation, 3 ml of solution was sampled and centrifuged to remove the photocatalysts with an EBA21 centrifuge (Hettich) at 14,000 rpm for 10 min. The supernatant solution was transferred to measure the retained amount of MO by absorption spectroscopy. The UV–vis absorption spectra were recorded on a Cary 50 Scan UV–vis spectrophotometer (Varian), and the absorbance of MO was measured at a wavelength of 504 nm, corresponding to maximum absorption wavelength of MO.

3. Results and discussion

3.1. Effects of SAM coating and graft polymerization of aniline on the preparation of PANI–TiO_2 hybrid composites

In the absence of TiO_2 nanoparticles, the polymerization of aniline was conducted, and the color of the growth solution system changed from light gray to dark green. However, in the presence of TiO_2 nanoparticles, color of the growth solution system changed from light blue to deep blue or green, depending on the initial concentration of aniline. This difference is indicative of the formation of the PANI/TiO_2 composite particles. However, we believe that the chemical stability of the PANI/TiO_2 composite particles is not so good because the PANI layer is just precipitated on the surface of neat-TiO_2 particles without a real chemical bounding. Thus, we employed the SAM technique and graft polymerization of aniline to prepare highly stable PANI–TiO_2 hybrid composites. Following the routes described in Section 2.2, we successfully synthesized SAM-coated TiO_2 nanoparticles and PANI/SAM-TiO_2 composites. In this preparation approach, γ-aminopropyltriethoxysilane was selected as a coupling agent, which has two functions from its functional groups. That is, a dense SAM was formed when it reacted with surface –OH groups on the vapor-treated TiO_2 nanoparticles in the first step. Because the attached silane chains possess a reactive end $-NH_2$ group, PANI chains can be grafted chemically on TiO_2 easily in the second step as illustrated in Fig. 1.

In the preparation of PANI/SAM-TiO_2 composites, the SAM coating is a very important step. Chemical anchoring of a SAM onto TiO_2 surface has been conformed by FTIR measurements. Fig. 2 compares the FTIR absorption spectra of neat-TiO_2, SAM-coated TiO_2, and PANI-grafted TiO_2 particles. The absorption band at 1402 cm^{-1} (spectrum 1 in Fig. 2) can be assigned to the in-plane bending vibration of O–H on the surface of TiO_2. The band at 1091 cm^{-1} attributed to the bending vibration of Ti–OH, is shifted to a lower wavenumber at 1000 cm^{-1} due to the creation of Ti–O–Si (spectrum 2). The almost disappearance of the band at 1402 cm^{-1} and the shifting of the 1091-cm^{-1} band in the SAM-coated TiO_2 demonstrate the chemical anchoring of

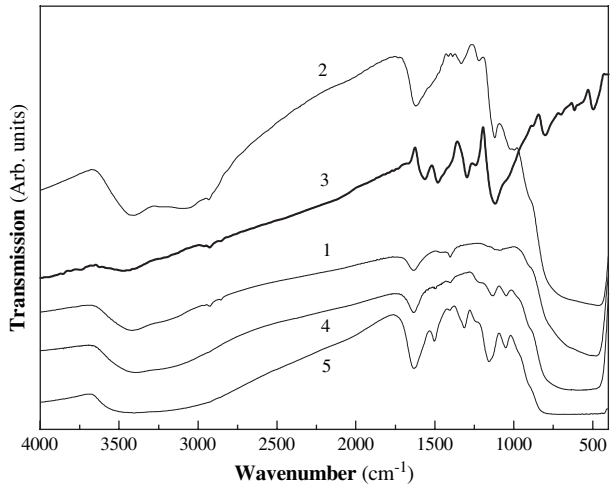

Fig. 2. FTIR spectra of neat-TiO_2 (1), SAM-coated TiO_2 (2), doped PANI (3), PANI-2.5/SAM-TiO_2 (4) and PANI-10/SAM-TiO_2 (5).

a SAM onto TiO_2 surface. In addition, the appearance of the peaks at 3089 and 2930 cm^{-1}, being assigned to the stretching vibrations of CH_2 in the SAM-coated TiO_2, is also indicative of the formation of a well-defined SAM layer. The new bands at 1526 cm^{-1} (as a shoulder of the 1618 cm^{-1} peak) and 1331 cm^{-1} are attributed to the bending vibration of CH_2 [24], and the new band at 1219 cm^{-1} is assigned to the stretching vibrations of N–H appear in the spectrum of the SAM-coated TiO_2 (spectrum 2), providing further evidences for this attachment.

Next to the SAM coating, a graft polymerization of aniline on the surface of SAM-coated particles results in the generation of PANI/SAM-TiO_2 composites, and thus most of FTIR characteristic bands for conventional doped PANI can be observed in the spectra of PANI/SAM-TiO_2 composites (spectra 3 and 4 in Fig. 2). As reported for conventional PANI [25,26], the main characteristic bands of doped PANI (spectrum 3 in Fig. 2) are assigned as follows: the band at 3474 cm^{-1} is attributable to N–H stretching mode, C=N and C=C stretching mode for the quinoid (Q) and benzenoid (B) rings occur at 1562 and 1480 cm^{-1}, the bands at about 1296 and 1241 cm^{-1} have been attributed to C–N stretching mode for benzenoid ring, while the peak at 1118 cm^{-1} is assigned to the in-plane bending vibration of C–H (mode of N=Q=N, Q=N^+H–B and B–N^+H–B), which is formed during protonation. However, the incorporation of nano-TiO_2 particles leads to the shift of some bands of PANI. For example, both of the bands at 1501 and 1403 cm^{-1}, corresponding to the stretching mode of C=N and C=C, are shifted to lower wavenumbers in the spectrum of PANI-10/SAM-TiO_2 sample. Meanwhile, the bands at 1311 and 1155 cm^{-1} (spectrum 4) correspond to C–N stretching mode for benzenoid ring and the in-plane bending vibration of C–H, respectively. These differences in the FTIR spectra can be mainly related to constrained growth and restricted modes of vibrations in PANI grown in the presence of TiO_2 [12]. By comparison with PANI-10/SAM-TiO_2, several characteristic bands of PANI grafted on the surface of the modified TiO_2 nanoparticles are slightly shifted to lower wavenumbers with a decreased intensity for the PANI-2.5/SAM-TiO_2 composites. The band at 1304 cm^{-1} attributable to C–N stretching mode for benzenoid ring is disappeared in the spectrum of PANI-2.5/SAM-TiO_2. Such peak shifting and intensity reducing are at least partially due to the restriction of PANI by TiO_2. High initial concentration of aniline in the polymerization solution results in thicker PANI layer on TiO_2 particles, leading to a weaker restriction of PANI by TiO_2.

3.2. Thermal stability and optical properties of PANI/TiO_2 nanocomposites

Li and coworkers have reported that an interaction between TiO_2 and PANI may weaken the interaction of inter-chains in PANI macromolecule, and increase the thermal degradation of PANI [25]. Fig. 3 depicts the TGA curves of PANI-10/neat-TiO_2 and PANI-10/SAM-TiO_2. The thermal decomposition curve (curve 1 in Fig. 3) of PANI-10/neat-TiO_2 shows a two-stage decomposition pattern. At temperatures lower than about 120 °C, the sample losses weight mainly be due to the loss of absorbed H_2O molecules, which becomes much slower from ~120 °C to ~240 °C. Due to the loss of dopants and the degradation of the polymer, the weight loss increases rapidly again beyond ~240 °C up to ~580 °C, at which all the organics are almost completely decomposed. With a comparison of TGA and DTG curves of PANI-10/SAM-TiO_2 and PANI-10/neat-TiO_2 composites, it is known that both composites yield similar thermal degradation behaviors at temperatures lower than about 300 °C and higher than 580 °C. However, the degradation of the polymer is markedly depressed at temperatures from ~300 °C to ~500 °C, being reflected by the appearance of a platform (curve 2) and much decreased values of the weight-loss derivability (curve 2′) at this temperature window. It is mainly attributed to the direct chemical bonding of PANI chains onto TiO_2 surface via self-assembling and graft polymerization with coupling agent. Because of the covalent bonding, there was only occurrence of partial degradation of the polymer for

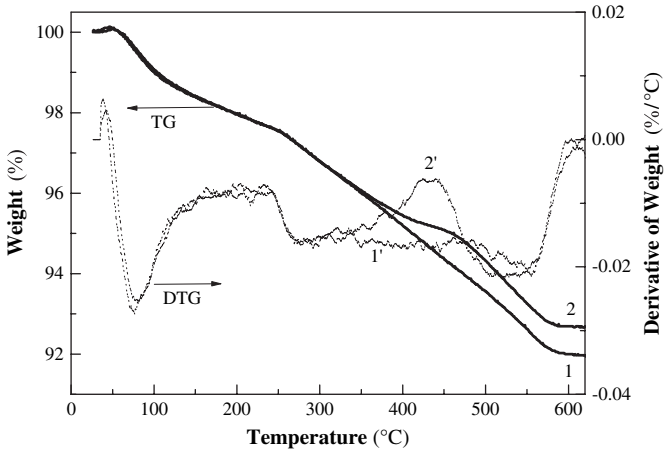

Fig. 3. TGA (1 and 2) and DTG (1′ and 2′) curves of PANI-10/neat-TiO_2 (1 and 1′) and PANI-10/SAM-TiO_2 (2 and 2′) composites.

PANI-10/SAM-TiO_2 at 420–450 °C, and complete degradation and decomposition of the grafted PANI and fixed coupling agent took place at 450–580 °C. In contrast, a platform showing a greater degradation rate was observed during the thermal degradation of polymer for PANI-10/neat-TiO_2 (curve 1′). Therefore, the PANI/SAM-TiO_2 composites exhibit improved thermochemical stability over the PANI/neat-TiO_2 composites. This increased thermochemical stability of PANI/SAM-TiO_2 is possibly attributed to the covalent bonding via PANI-grafting onto the TiO_2 surface.

Moreover, we have measured the amount of PANI grafted on the surface of TiO_2 particles with the aid of TG analysis. The amounts of grafted PANI are estimated as 3.0% for PANI-2.5/SAM-TiO_2, 6.1% for PANI-10/SAM-TiO_2, and 6.7% for PANI-10/neat-TiO_2. This suggests that the average thickness of the grafted PANI layer is mainly determined by the monomer concentration used in the preparation process.

The UV–vis-diffuse reflectance spectra of neat-TiO_2, PANI/neat-TiO_2 and PANI/SAM-TiO_2 were measured as shown in Fig. 4. The band-gap energy of anatase TiO_2 is about 3.2 eV, corresponding to a threshold wavelength of 387.5 nm. Thus, there is no absorption beyond the wavelength of 380 nm for neat-TiO_2 (curve 1 in Fig. 4). However, a marked absorption is observed in the region of 380–800 nm when TiO_2 nanoparticles were capped with PANI (curves 2–4). The absorption peak at 443 nm can be assigned to the localized polarons in protonated PANI [27,28]. It is noted that curves 3 and 4 in Fig. 4 are almost same. This is rational because the grafted PANI layers for these two samples are almost the same and the absorption in the visible region is mainly contributed from the coated PANI layer no matter with the way that the PANI layer is chemically or physically bonded. A comparison between curves 2 and 3 suggests that a thinner layer of PANI produces weaker absorption. Thus, the absorption of the PANI/TiO_2 composites in the visible region is certainly attributed to the PANI layer, favoring the enhancement of photocatalytic activity of the composites under sunlight.

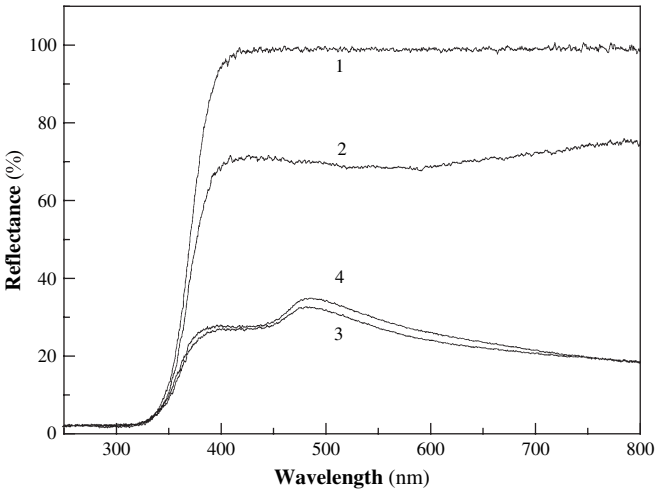

Fig. 4. UV–vis-diffuse reflectance spectra of neat-TiO_2 (1), PANI-2.5/SAM-TiO_2 (2), PANI-10/SAM-TiO_2 (3) and PANI-10/neat-TiO_2 (4).

3.3. Morphology of PANI/TiO_2 nanocomposites

Because the morphology and aggregation state of the nanoparticles will influence their specific surface area and then photocatalytic activity, we observed the morphology of the prepared samples. Fig. 5 shows the TEM photographs of neat-TiO_2, SAM-coated TiO_2 and PANI-2.5/SAM-TiO_2. The PANI/TiO_2 composite and SAM-coated TiO_2 nanoparticles are rather spherical in shape, being similar to that of neat-TiO_2. However, the shape of PANI synthesized under the same condition in the absence of TiO_2 nanoparticles is fibular (not shown). This indicates that the TiO_2 nanoparticles have a nucleation effect for the graft polymerization of aniline in the preparation process.

3.4. Photocatalytic activities of PANI/TiO_2 nanocomposites

TiO_2 is well studied as a photocatalyst to decompose organic and inorganic molecules. The mechanism is believed to involve the absorption of a UV photon by TiO_2 to produce an electron–hole pair. These react with water to yield hydroxyl and superoxide radicals, which oxidize and mineralize the organic and inorganic molecules. However, because the forbidden band gap of TiO_2 is 3.2 eV, only UV light can be utilized, with poor photocatalytic efficiency under sunlight. One solution to overcome this shortcoming is using a dye with narrow forbidden band gap as sensitizer, so as to enhance the photocatalysis efficiency of TiO_2. PANI has a forbidden band gap of 2.8 eV, showing strong absorption in the region of visible light. Hence, it may function as a sensitizer to TiO_2.

Fig. 6 gives a schematic energy diagram, where the energies of the highest occupied molecular orbital (HOMO) and the lowest unoccupied molecular orbital (LUMO) were cited from Refs. [24,29]. When PANI/TiO_2 nanocomposites are illuminated under sunlight, both TiO_2 and PANI absorb the photons at their interface, then charge separation occurs at the interface. Since the conduction band of TiO_2 and the LUMO level of the PANI are well matched for the charge transfer, the generated electrons by inducing PANI can be transferred to the conduction band of TiO_2, enhancing the charge separation and in turn promoting the photocatalytic ability of the photocatalyst.

Prior to the photocatalytic experiment under sunlight, we carried out similar experiment under UV irradiation using a 20-W mercury lamp as UV light source. It was found that the neat-TiO_2 particles yielded photocatalytic activity very slightly better than the PANI-coated TiO_2 particles under UV irradiation (not shown here). However, the latter yielded photocatalytic activity slightly better than the former. Fig. 7 gives the kinetic data for the degradation of MO in aqueous solution in the presence of neat-TiO_2 and PANI-2.5/SAM-TiO_2 composite as photocatalyst under sunlight. Although the difference between curves 1 and 2 in Fig. 7 is rather small, the photocatalytic degradation rate of MO over PANI-2.5/SAM-TiO_2 is faster than that over neat-TiO_2. Therefore, the PANI/TiO_2 composites have better photocatalytic activity under

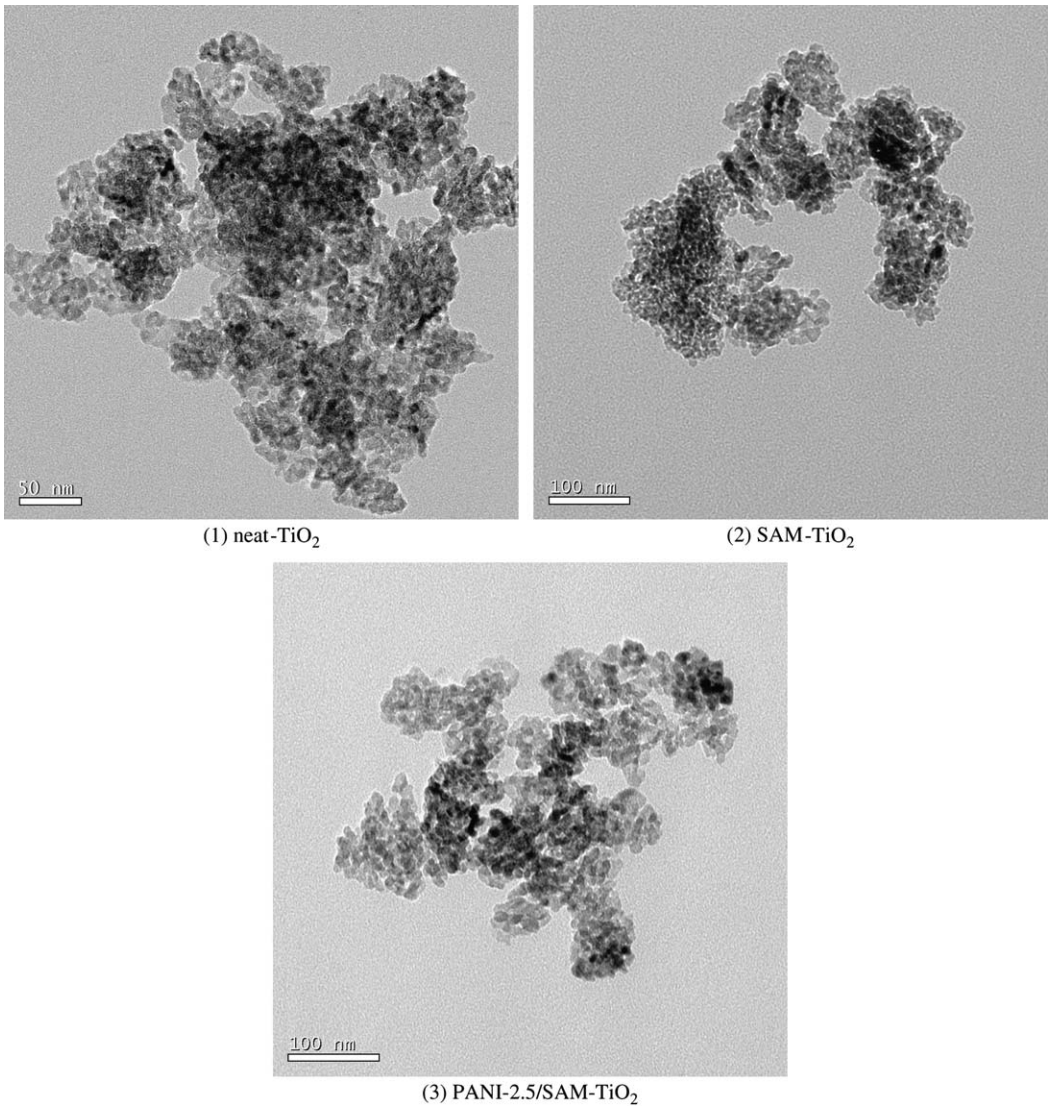

Fig. 5. TEM images of neat-TiO_2 (1), SAM-coated TiO_2 (2) and PANI-2.5/SAM-TiO_2 (3) nanoparticles.

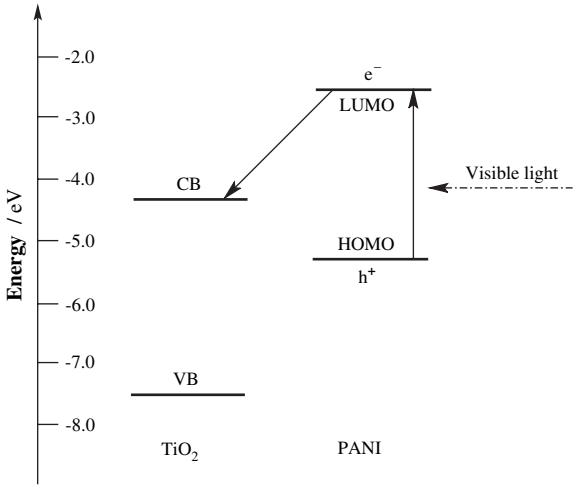

Fig. 6. Schematic energy diagram for the composite of PANI and TiO_2.

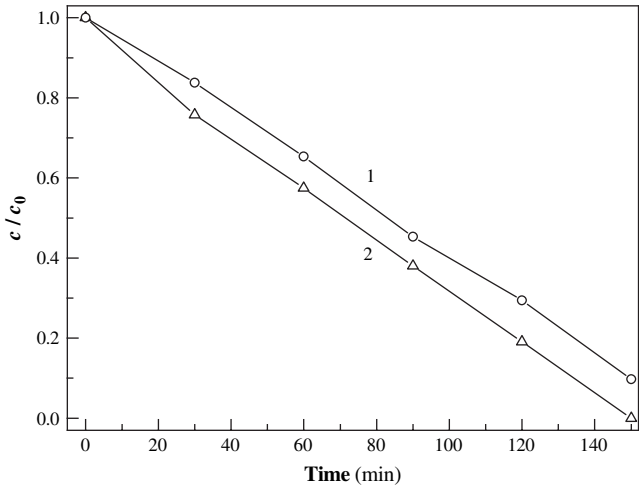

Fig. 7. Kinetic data for the degradation of aqueous MO ($c_0 = 10$ mg L^{-1}) irradiated under sunlight, over the photocatalyst of neat-TiO_2 (1) and PANI-2.5/SAM-TiO_2 (2).

sunlight, as anticipated from the energy diagram (Fig. 6). Because the improvement in the photocatalytic activity is limited, we have not observed marked difference between PANI-2.5/SAM-TiO_2 and PANI-2.5/neat-TiO_2. In addition, the photocatalytic activity of PANI-10/SAM-TiO_2 was found to be poorer than that of PANI-2.5/SAM-TiO_2, indicating that a thick PANI layer is unfavorable to the photocatalytic activity of the composites.

4. Conclusion

Nanocrystalline TiO_2 particles were successfully capped with PANI through the self-assembled aminopropylsilane monolayer and chemical oxidative graft polymerization. In the synthesis approach, selection of γ-aminopropyltriethoxysilane as a coupling agent was an important strategy. This coupling agent was used to easily form a dense SAM, which was further adopted to the grafting of PANI. The successful SAM coating and grafting of PANI molecules onto the surface of TiO_2 nanoparticles were confirmed by the analysis results of FTIR, TGA and UV–vis-diffuse reflectance spectroscopy. The combination of SAM coating and surface PANI-grafting improved the thermal stability of the PANI/TiO_2 composites, because of the covalent bonding between PANI chains and TiO_2 particles. The PANI/TiO_2 composites showed absorption in the visible light region, and this would favor the photocatalytic activity of TiO_2 under sunlight. As expected, the PANI/SAM-TiO_2 composites exhibited better photocatalytic activity in photocatalytic degradation of MO under sunlight, compared with the neat-TiO_2 nanoparticles without any surface modification, due to the sensitizing effect of PANI.

Acknowledgments

We gratefully acknowledge the financial supports from the National Science Foundation of China (grants no. 30571536), from the Scientific Research Foundation for the Returned Overseas Chinese Scholars from State Education Ministry of China, and from Hubei Key Laboratory for Catalysis and Material Science in South-Central University for Nationalities.

References

[1] Gao M, Richer B, Kirstein S. Adv Mater 1997;9:802–5.
[2] Cassagneau T, Mallouk TE, Fendler JH. J Am Chem Soc 1998;120:7848–59.
[3] Gangopadhyay R, De A. Chem Mater 2000;12:608–22.
[4] Schnitzler DC, Meruvia MS, Hummelgen IA, Zarbin AJG. Chem Mater 2003;15:4658–65.
[5] Maeda S, Corradi R, Armes SP. Macromolecules 1995;28:2905–11.
[6] McCarthy GP, Armes SP, Greaves SJ, Watts JF. Langmuir 1997;13:3686–92.
[7] Ogura K, Endo N, Nakayama M. J Electrochem Soc 1998;145:3801–9.
[8] Xia HS, Wang Q. Chem Mater 2002;14:2158–62.
[9] Deng JG, Ding XB, Zhang WC, Peng YX, Wang JH, Long XP, et al. Polymer 2002;43:2179–84.
[10] Xia HS, Wang Q. J Appl Polym Sci 2003;87:1811–7.
[11] Yoneyama H. Adv Mater 1993;5:394–6.
[12] Somani PR, Marimuthu R, Mulik UP, Sainkar SR, Amalnerkar DP. Synth Met 1999;106:45–52.
[13] Zhang LJ, Wan MX. J Phys Chem B 2003;107:6748–53.
[14] Xiong SX, Wang Q, Xia HS. Synth Met 2004;146:37–42.
[15] Weck M, Jackiw JJ, Rossi RR, Weiss PS, Grubbs RH. J Am Chem Soc 1999;121:4088–9.
[16] Nuß S, Böttcher H, Wurm H, Hallensleben ML. Angew Chem Int Ed 2001;40:4016–8.
[17] Jordan R, West N, Ulman A, Chou YM, Nuyken O. Macromolecules 2001;34:1606–11.
[18] Mandal TK, Fleming MS, Walt DR. Nano Lett 2002;2:3–7.
[19] Li ZF, Swihart MT, Ruckenstein E. Langmuir 2004;20:1963–71.
[20] Lee LS, Cho MS, Choi HJ. Polymer 2005;46:1317–21.
[21] Ruckenstein E, Li ZF. Adv Colloid Interface Sci 2005;13:43–63.
[22] Li ZF, Ruckenstein E. Macromolecules 2002;35:9506–12.
[23] Marutani E, Yamamoto S, Ninjbadgar T, Tsujii Y, Fukuda T, Takano M. Polymer 2004;45:2231–5.
[24] Senadeera GKR, Kitamura T, Wadab Y, Yanagida S. J Photochem Photobiol A 2004;164:61–6.
[25] Li XW, Wang GC, Lu DM. Appl Surf Sci 2004;229:395–401.
[26] Dimitriev OP. Macromolecules 2004;37:3388–95.
[27] Yue J, Wang ZH, Cromack KR, Epstein AJ, MacDiarmid AG. J Am Chem Soc 1991;113:2665–71.
[28] Athawale AA, Kulkarni MV, Chabukswar VV. Mater Chem Phys 2002;73:106–10.
[29] Li Y, Hagen J, Haarer D. Synth Met 1998;94:273–7.